Electronic Supplementary Information
for

# A Hexanuclear Gold Carbonyl Cluster

Sonia Martínez-Salvador, Larry R. Falvello, Antonio Martín, and Babil Menjón*

## Experimental Section

# 1. EXPERIMENTAL SECTION

**General Procedures and Materials.** Unless otherwise stated, the reactions and manipulations were carried out under purified argon using Schlenk techniques. Solvents were dried using an MBraun SPS-800 System. Solutions of the parent compound $CF_3AuCO$ (**1**) were obtained as described elsewhere and further used without effecting isolation.[S1] The $[PPh_4]Br$ salt (Aldrich) was purchased and used as received. Elemental analyses were carried out using a Perkin Elmer 2400 CHNS/O Series II microanalyzer. IR spectra of KBr discs were recorded on the following Perkin-Elmer spectrophotometers: 883 (4000–200 $cm^{-1}$) or Spectrum One (4000–350 $cm^{-1}$). To avoid decomposition, the IR spectra of the thermally unstable hexanuclear aggregate **4** containing highly labile CO ligands were recorded by using an attenuated total reflectance (ATR) device operating in the 4000–250 $cm^{-1}$ range. Consequently, the ν(Au–Br) frequency—presumably lying below the operating range—was not determined in this case. NMR spectra were recorded on any of the following spectrometers: Bruker ARX 300 or Bruker ARX 400. Unless otherwise stated, the spectroscopic measurements were carried out at room temperature. Chemical shifts of the measured nuclei ($\delta$ in ppm) are given with respect to the standard references in use: $SiMe_4$ ($^{13}C$) and $CFCl_3$ ($^{19}F$). NMR parameters associated with the $[PPh_4]^+$ cation are unexceptional and are therefore omitted.

**Synthesis of $[PPh_4][CF_3AuBr]$ (2)**: To an *in situ* prepared colorless solution of compound **1** (0.30 mmol) in $CH_2Cl_2$/*n*-hexane (10 and 20 $cm^3$, respectively) at 0 °C was added $[PPh_4]Br$ (0.11 g, 0.27 mmol). A white solid formed, which was filtered, washed with *n*-hexane and vacuum dried (**2**: 0.14, 0.20 mmol, 74% yield with respect to the limiting reagent bromide). $^{13}C\{^1H\}$ NMR (100.577 MHz, $CD_2Cl_2$): $\delta = 151.2$ ppm (q, $^1J(^{19}F,^{13}C) = 347$ Hz; $CF_3$); $^{19}F$ NMR (282.231 MHz, $CD_2Cl_2$): $\delta = -22.01$ ppm (s; $CF_3$); IR (KBr): $\tilde{\nu}_{max} = 1585$ (m), 1482 (s), 1441 (vs), 1435 (vs), 1397 (w), 1339 (w), 1314 (w), 1185 (w), 1165 (w), 1119 (vs), 1108 (vs), 1027 (w), 983 (vs), 982 (vs), 802 (w), 755 (s), 723 (vs), 689 (vs), 616 (w), 526 (vs), 455 (w), 443 (w), 431 (w), 276 $cm^{-1}$ (s; Au–Br); elemental analysis calcd (%) for $C_{25}H_{20}AuBrF_3P$: C 43.8, H 2.9; found: C 43.6, H 2.8.

Single crystals suitable for X-ray diffraction purposes were obtained by slow diffusion of a *n*-hexane (10 cm$^3$) layer into a solution of 10 mg of compound **2** in $CH_2Cl_2$ (3 cm$^3$) at 4 °C.

**Synthesis of [$PPh_4$][Br($AuCF_3$)$_2$] (3)**: To an *in situ* prepared colorless solution of compound **1** (0.30 mmol) in $CH_2Cl_2$/*n*-hexane (10 and 20 cm$^3$, respectively) at 0 °C was added [$PPh_4$]Br (50 mg, 0.12 mmol). A white solid formed, which was filtered, washed with *n*-hexane and vacuum dried (**3**: 0.1 g, 0.105 mmol, 87% yield with respect to the limiting reagent bromide). $^{13}C\{^1H\}$ NMR (100.577 MHz, $CD_2Cl_2$, −20 ºC): $\delta = 144.9$ ppm (q, $^1J(^{19}F,^{13}C) = 347$ Hz; $CF_3$); $^{19}F$ NMR (282.231 MHz, $CD_2Cl_2$, −20 ºC): $\delta = -22.65$ ppm (s; $CF_3$); IR (KBr): $\tilde{\nu}_{max} = 1585$ (w), 1483 (m), 1441 (s), 1435 (s), 1339 (w), 1314 (w), 1261 (w), 1189 (w), 1164 (w), 1110 (vs), 1005 (vs), 987 (vs), 803 (w), 754 (m), 722 (vs), 689 (vs), 615 (w), 527 (vs), 455 (w), 432 (w), 271 cm$^{-1}$ (s; Au–Br); elemental analysis calcd (%) for $C_{26}H_{20}Au_2BrF_6P$: C 32.8, H 2.1; found: C 32.8, H 2.2.

Single crystals of **3**·$CH_2Cl_2$ suitable for X-ray diffraction purposes were obtained by slow diffusion of a *n*-hexane (10 cm$^3$) layer into a solution of 10 mg of compound **3** in $CH_2Cl_2$ (3 cm$^3$) at 4 °C.

**Synthesis of [$PPh_4$]$_2$[$Au_6(CF_3)_6Br_2(CO)_2$] (4)**: To an *in situ* prepared colorless solution of compound **1** (0.30 mmol) in $CH_2Cl_2$/*n*-hexane (10 and 20 cm$^3$, respectively) at −30 °C was added [$PPh_4$]Br (31 mg, 75 μmol). A white solid formed, which was filtered, washed with *n*-hexane and vacuum dried (**4**: 50 mg, 20 μmol, 53% yield with respect to the limiting reagent bromide). $^{19}F$ NMR (282.231 MHz, $CD_2Cl_2$): $\delta = -22.65$ (s, 2F; $CF_3$ in component **3**), −30.81 ppm (s, 1F; $CF_3$ in component **1**); IR (ATR): $\tilde{\nu}_{max} = 2171$ (s; C≡O), 1585 (w), 1484 (w), 1436 (s), 1188 (w), 1170 (w), 1130 (s), 1106 (vs), 1079 (s), 996 (vs), 987 (vs), 852 (w), 755 (s), 746 (w), 723 (vs), 704 (w), 687 (vs), 613 (w), 523 (vs), 447 (w), 430 (w), 389 (w), 361 cm$^{-1}$ (w); elemental analysis calcd (%) for $C_{56}H_{40}Au_6Br_2F_{18}O_2P_2$: C 27.0, H 1.6; found: C 27.0, H 1.4.

Single crystals suitable for X-ray diffraction purposes were obtained by slow diffusion of a *n*-hexane (10 cm$^3$) layer into a solution of 10 mg of compound **4** in $CH_2Cl_2$ (3 cm$^3$) at −60 °C.

# 2. X-RAY STRUCTURE DETERMINATIONS

## 2.1. Data Collection

Crystal data and other details of the structure analyses are presented in Table S1. Suitable crystals for X-ray diffraction studies, obtained as indicated in the corresponding experimental entry, were mounted at the end of a quartz fiber in a random orientation and held in place with fluorinated oil. Data collection was performed at 100 K temperature on an Oxford Diffraction Xcalibur CCD diffractometer using graphite monochromated Mo-Kα radiation ($\lambda = 71.073$ pm) with a nominal crystal to detector distance of 5.0 cm. The diffraction frames were integrated and corrected for absorption by using the CrysAlis RED package.[S2] Lorentz and polarization corrections were applied.

## 2.2. Crystal Structure Analyses of Compounds 2 and 4

The structures of compounds **2** and **4** were solved by direct methods and refined by full-matrix least squares on $F^2$ with SHELXL-97.[S3] All non-hydrogen atoms were assigned anisotropic displacement parameters and refined freely. All hydrogen atoms were constrained to idealized geometries and assigned isotropic displacement parameters equal to 1.2 times the $U_{\text{iso}}$ values of their attached parent atoms. In the structure of compound **2**, final difference electron density maps showed three peaks above 1 e Å$^{-3}$ (max. 1.29; min. dif. hole − 1.06) very close to the Au atom. In the structure of compound **4**, final difference electron density maps showed 17 peaks above 1 e Å$^{-3}$ (max. 3.14; min. dif. hole − 2.26) near the Au atoms. Full-matrix least-squares refinement of these models against $F^2$ converged to final residual indices given in Table S1.

## 2.3. Crystal Structure Analysis of 3·$CH_2Cl_2$

*2.3.1. Data Integration:* It was possible to index the diffraction pattern using three domains with the same monoclinic unit cell. Three domains gave what we considered to be good cell parameters, as judged for example by the values of the 90° angles when symmetry constraints were not used. A fourth domain was located but did not index the pattern as well, and for the fourth domain one of the 90º unit-cell angles was refined consistently with values of several tenths of a degree variation from its required value, in the absence of constraints.

Several strategies were attempted for the integration of the data. In the first instance, the data were integrated using the automatic procedure of the diffractometer, which gives just one unit cell, one domain, and one set of diffraction data. The data were also integrated using the three principal domains that had given acceptable unit-cell parameters. This integration involved deconvolution of the overlapped peaks in a single-pass integration procedure. Both combined data (Shelx HKLF 5) and individual domain data sets (Shelx HKLF 4) were produced in this procedure. Another attempt involved a similar one-pass integration, but using the fourth domain as well as the three principal domains. A four-domain multi-pass integration was also performed.

After refining with all of these data sets and with others that resulted from several alternative integration strategies, we concluded that the best refinement available for this sample was that which used the combined data (HKLF 5) from the three-domain single-pass integration.

*2.2.2 Structure solution and refinement:* The crystallographic asymmetric unit consists of one $CH_2Cl_2$ molecule, one $[PPh_4]^+$ cation, and what is stoichiometrically one $[Br(AuCF_3)_2]^-$ anion.

The structure was solved independently by direct methods[S4] and by the method incorporated in the program ShelxT.[S5] The same result is obtained by both methods, and reveals a structure in which the cation and the solvent molecule are ordered, while the anion site is highly disordered.

The anion is distributed over four orientations within a cavity located on a crystallographic inversion center at (½, 0, ½) and symmetry-related sites. The particulars of the disorder assembly and the distribution of the disorder groups required special treatment.[S6]

A simultaneously-occupied pair of V-shaped anions are located on opposite sides of the center of symmetry, but are not related by it. As seen in Figure S1, these two anions lie in planes nearly perpendicular to each other. The center of inversion (½, 0, ½) lies at the midpoint of the Br1···Br1A vector.

It was necessary to apply restraints to geometrical and displacement parameters, and for this disorder assembly the use of restraints required special treatment of the symmetry element. All of the atomic sites in Figure S1 are general positions. All have site occupancy of 0.5. The atoms shown in Figure S1 are those included for the anion in the atoms list for one asymmetric unit. However, some of the sites are symmetry relatives of others. For example, C1 ($x$, $y$, $z$) and C1A ($1-x$, $-y$, $1-z$) are related by the inversion center at (½, 0, ½). In order to be able to apply restraints involving atoms that are not related by symmetry (*e.g.,* F3 and F3A) and atoms that are so related, using the features of the refinement program ShelxL2014/7, it was convenient to include explicit atomic positions for the symmetry related pair C1 and C1A. The coordinates of C1 at ($x$, $y$, $z$) and those of C1A at ($1-x$, $-y$, $1-z$) were constrained to this symmetry relationship using the free variable feature of the program. The same treatment was given to the pairs F1/F1A and F2/F2A. Br1 of one of the anions was also so related to Br1A of the other. For the second anion disorder group, the same treatment was applied to the pairs C2/C2A, F4/F4A and F5/F5A. *N.b.,* F6 and F6A, like F3 and F3A, are not related to each other by symmetry.

The structural model includes the center of symmetry, so the pair of V-shaped anions shown in Figure S1 is present in the disorder assembly along with its inversion-related congener.

All non-hydrogen atomic sites in the structure were observed either in the initial solution of the structure or in difference maps. Hydrogen atoms were placed in calculated positions (C–H = 93 pm for the phenyl rings and 97 pm for $CH_2Cl_2$) and refined as riding atoms with $U_{iso}(H) = 1.2U_{eq}(C)$.

The pejorative effects of the multi-domain diffraction pattern obliged us to use restraints to achieve a convergent refinement. For the $CF_3$ groups, after the initial location of the F atoms in difference maps, the geometry of these groups was idealized. Then in the refinement, explicit restraints were used for the C–F [132.8(20) pm] and F···F [212.5(20) pm] distances. To avoid exaggerated tilting of the $CF_3$ groups, similarity restraints were applied to the three Au···F distances for each. Similarity restraints were also applied to the four independent Au···C distances.

Displacement parameters were also restrained. Rigid-bond restraints based on the Hirshfeld model[S7] were used for the anisotropic displacement parameters of the 1,2- and 1,3- pairs of non-H atoms in the cation. For the $CF_3$ groups, both the Hirshfeld-model restraints and the Thorn-Dittrich-Sheldrick "enhanced rigid-bond" restraints, which require the relative motion of two atoms to be perpendicular to the vector joining them,[S8] were applied. The resulting refinement was convergent, but atom F6A had a non-positive-definite displacement tensor, so in the final, convergent refinement F6A was further subjected to restraints to isotropic behavior. As a result, it emerged positive-definite but with a rather oblate displacement ellipsoid (Figure S1). We prefer to retain this model, which is physically realistic but still belies the underlying problem in the data, rather than apply further adjustments, which would be purely cosmetic in nature.

The final refinement converged with the residuals given in Table S1.

**Table S1.** Crystal data and structure refinement for compounds **2**, **3**·$CH_2Cl_2$ and **4**.

| | **2** | **3**·$CH_2Cl_2$ | **4** |
|---|---|---|---|
| formula | $C_{25}H_{20}AuBrF_3P$ | $C_{27}H_{22}Au_2BrCl_2F_6P$ | $C_{56}H_{40}Au_6Br_2F_{18}O_2P_2$ |
| $M_t$ (g mol$^{-1}$) | 685.26 | 1036.16 | 2490.44 |
| $T$ (K) | 100(2) | 100(2) | 100(2) |
| $\lambda$ (pm) | 71.073 | 71.073 | 71.073 |
| crystal system | orthorhombic | monoclinic | monoclinic |
| space group | $P2_12_12_1$ | $P2_1/n$ | $C2/m$ |
| $a$ (pm) | 837.81(2) | 1122.08(16) | 1161.00(3) |
| $b$ (pm) | 1438.27(2) | 1616.8(3) | 2390.64(7) |
| $c$ (pm) | 1931.53(3) | 1703.1(3) | 1115.68(3) |
| $\beta$ (deg) | 90.00 | 108.049(19) | 97.975(3) |
| $V$ (nm$^3$) | 2.32749(7) | 2.9377(9) | 3.06666(15) |
| $Z$ | 4 | 4 | 2 |
| $\rho$ (g cm$^{-3}$) | 1.956 | 2.343 | 2.697 |
| $\mu$ (mm$^{-1}$) | 8.140 | 11.628 | 15.749 |
| $F$(000) | 1304 | 1920 | 2256 |
| $\theta$ range (deg) | 4.24–28.89 | 4.24–27.49 | 4.13–28.87 |
| final $R$ indices [$I > 2\sigma(I)$]$^a$ | | | |
| $R_1$ | 0.0234 | 0.0813 | 0.0337 |
| $wR_2$ | 0.0542 | 0.2471 | 0.0849 |
| $R$ indices (all data) | | | |
| $R_1$ | 0.0253 | 0.1135 | 0.0432 |
| $wR_2$ | 0.0549 | 0.2633 | 0.0877 |
| goodness-of-fit$^b$ on $F^2$ | 1.062 | 1.060 | 1.016 |
| CCDC no.$^c$ | 1049919 | 1049920 | 1049921 |

[a] $R_1 = \sum(|F_o| - |F_c|) / \sum|F_o|$; $wR_2 = [\sum w(F_o^2 - F_c^2)^2 / \sum w(F_o^2)^2]^{1/2}$. [b] Goodness-of-fit = $[\sum w(F_o^2 - F_c^2)^2 / (n_{obs} - n_{param})]^{1/2}$. [c] The given CCDC nos. contain the supplementary crystallographic data; these data can be obtained free of charge from The Cambridge Crystallographic Data Centre *via* www.ccdc.cam.ac.uk/data_request/cif.

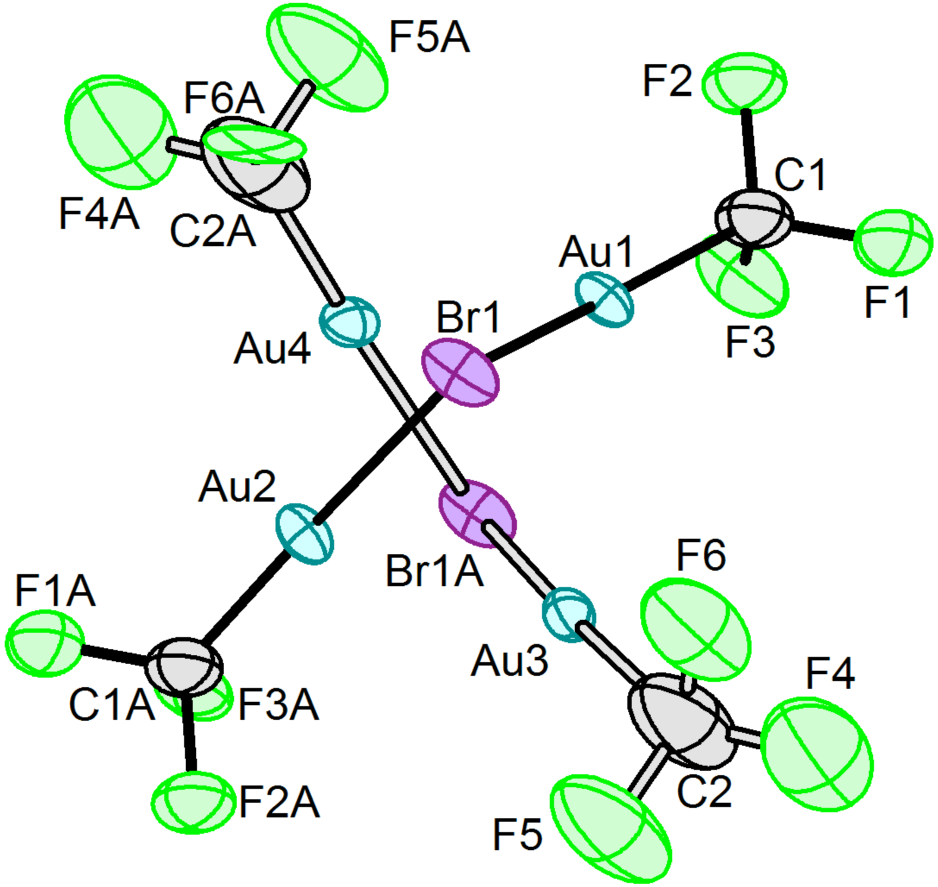

**Figure S1.** The anion sector of one asymmetric unit of the structure of **3**·$CH_2Cl_2$, with atomic sites represented by their 50% probability ellipsoids. This graphic represents one disorder group.

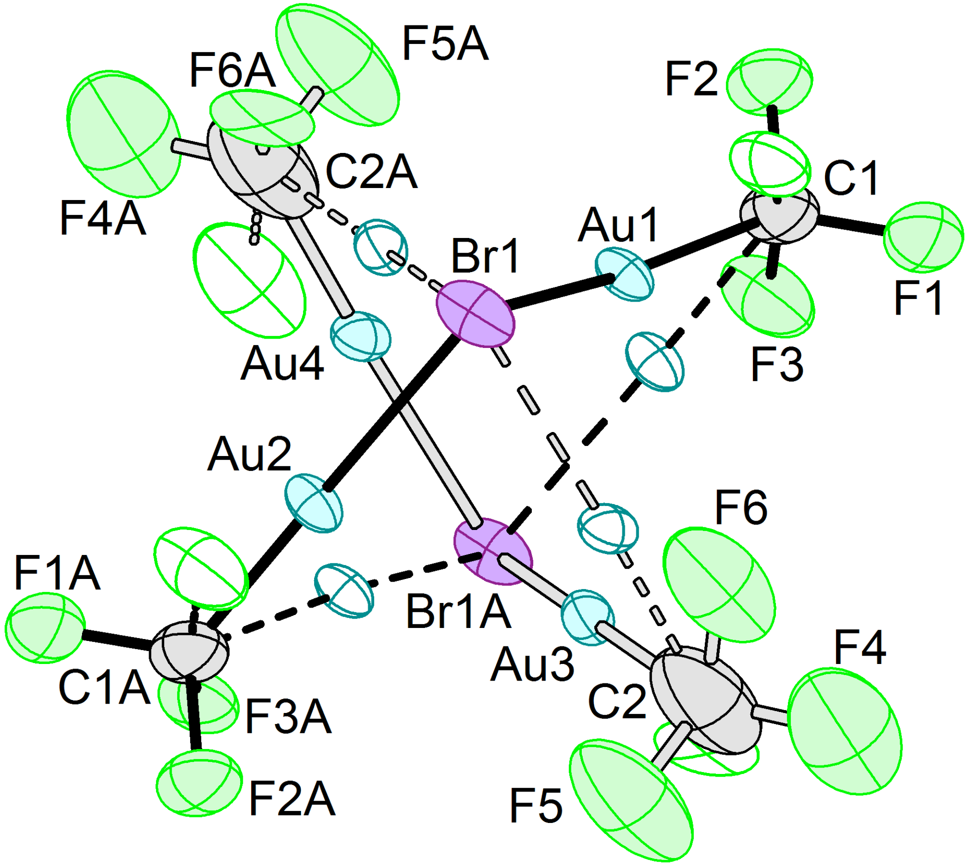

**Figure S2.** Atomic sites of the entire disorder assembly for the anion sector of the structure of **3**·$CH_2Cl_2$, with atomic sites represented by their 50% probability ellipsoids.

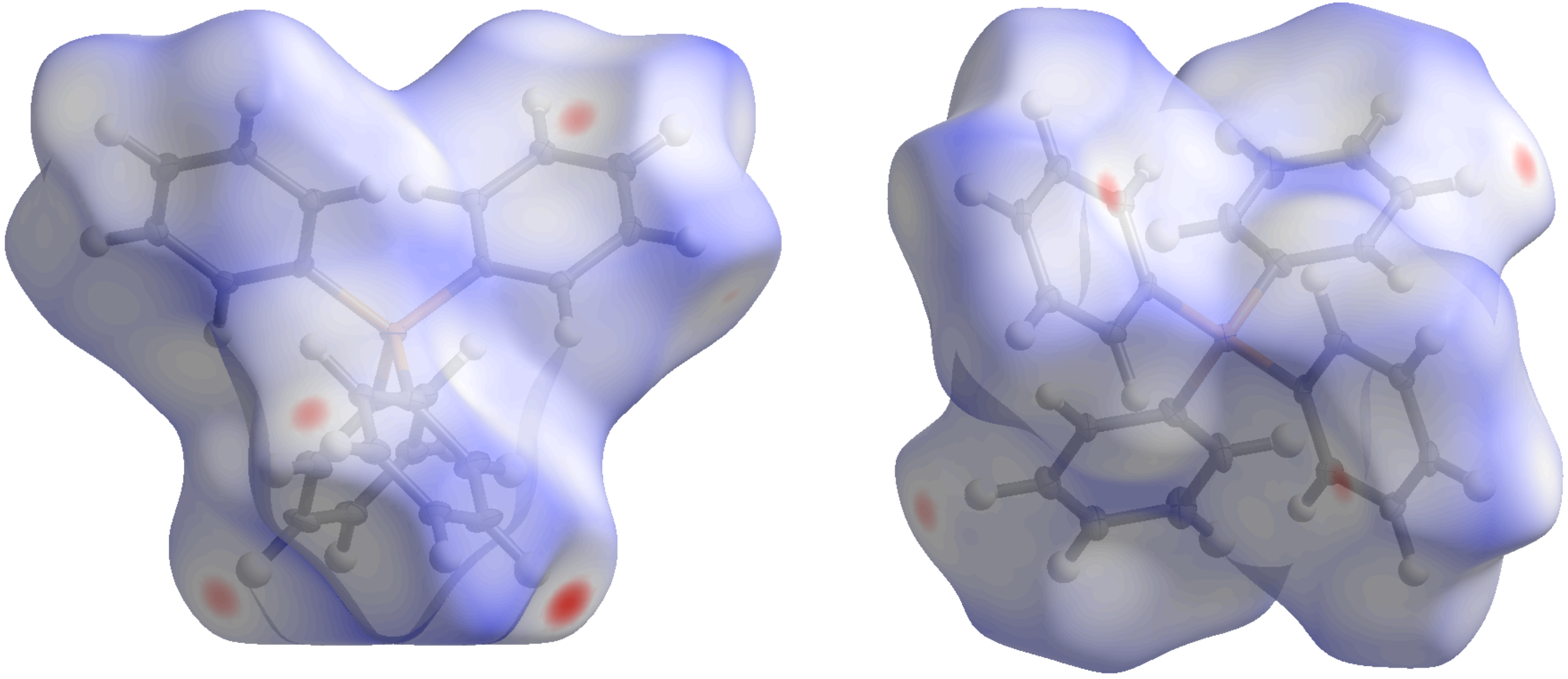

**Figure S3.** Three-dimensional Hirshfeld surface (HS) for the $[PPh_4]^+$ cation in the crystal of **4**, with two complementary orientations given for a better portrayal. The HS was mapped[S9] with $d_{norm}$ and generated using Crystal Explorer 3.1.[S10]

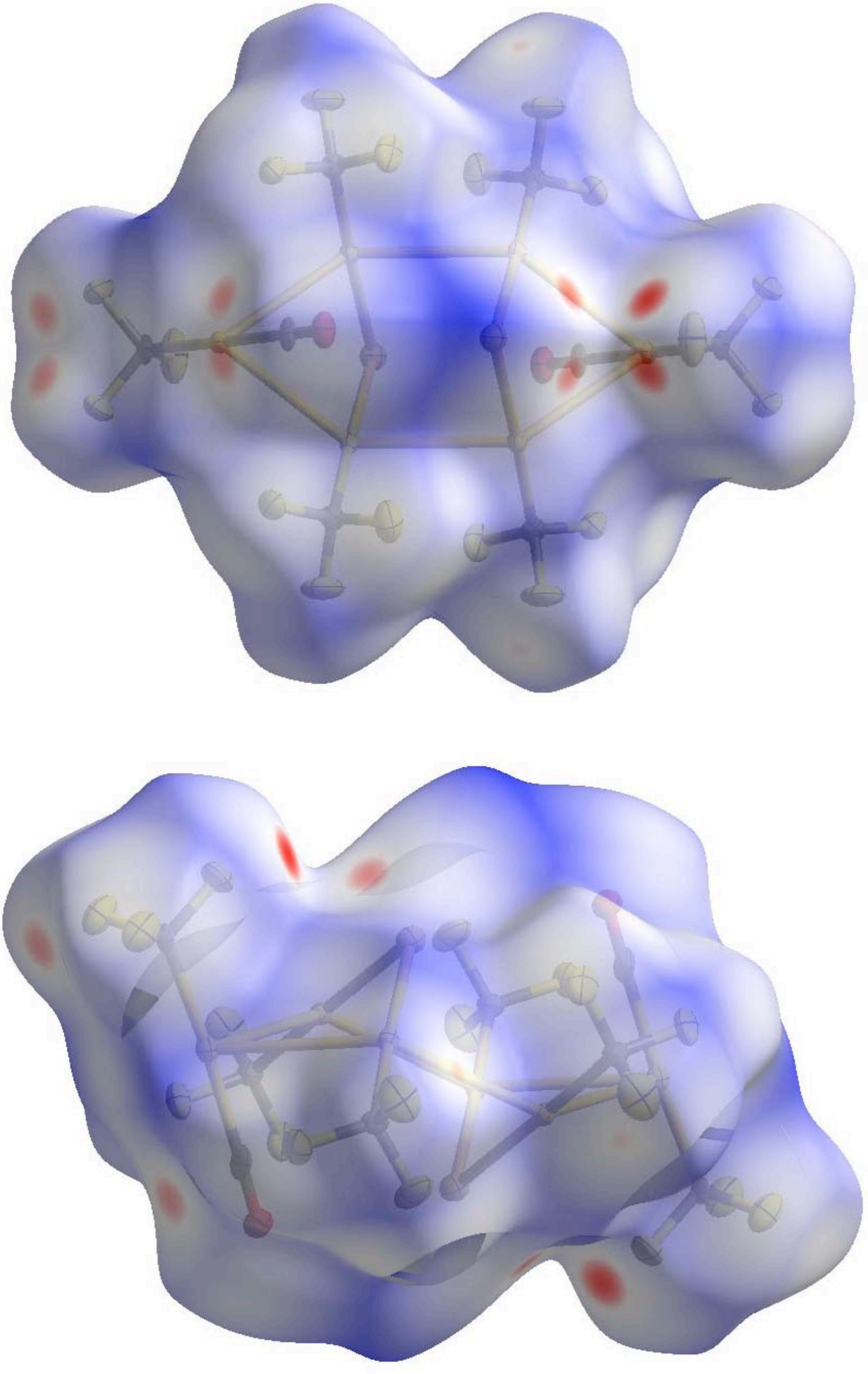

**Figure S4.** Three-dimensional Hirshfeld surface (HS) for the $[Au_6(CF_3)_6Br_2(CO)_2]^{2-}$ anion in the crystal of **4**, with two complementary orientations given for a better portrayal. The HS was mapped[S9] with $d_{norm}$ and generated using Crystal Explorer 3.1.[S10]

## References

S1 S. Martínez-Salvador, L. R. Falvello, A. Martín and B. Menjón, *Chem. Eur. J.*, 2013, **19**, 14540–14552. S. Martínez-Salvador, J. Forniés, A. Martín and B. Menjón, *Angew. Chem. Int. Ed.*, 2011, **50**, 6571–6574.

S2 *CrysAlis RED: Program for X-ray CCD camera data reduction*, Version 1.171.32.19, Oxford Diffraction Ltd., Oxford, UK, 2008.

S3 G. M. Sheldrick, *SHELXL-97: Program for the Refinement of Crystal Structures from Diffraction Data*, University of Göttingen, Göttingen (Germany), 1997.

S4 A. Altomare, G. Cascarano, C. Giacovazzo, A. Guagliardi, M. C. Burla, G. Polidori and M. Camalli, *J. Appl. Cryst.,* 1994, **27**, 435.

S5 G. M. Sheldrick, *Acta Crystalogr., Sect A,* 2015, **71**, 3–8.

S6 The terms "disorder assembly" and "disorder group" as recognized by the International Union of Crystallography are defined in: Core dictionary (coreCIF) version 2.4.5 (http://www.iucr.org/__data/iucr/cifdic_html/1/cif_core.dic/).

S7 F. L. Hirshfeld, *Acta Crystallogr., Sect A,* 1976, **32**, 239–244.

S8 A. Thorn, B. Dittrich and G. M. Sheldrick, *Acta Crystallogr., Sect. A,* 2012, **68**, 448–451

S9 M. A. Spackman and J. J. McKinnon, *CrystEngComm*, 2002, **4**, 378–392.

S10 CrystalExplorer (Version 3.1), S. K. Wolff, D. J. Grimwood, J. J. McKinnon, M. J. Turner, D. Jayatilaka and M. A. Spackman, University of Western Australia, 2012.